

## Supplementary Information

### A Highly Reversible Sodium Metal Anode via Mitigating Electrodeposition Overpotential

Pan Xu,<sup>‡</sup> Xin Li,<sup>‡</sup> Mei-Yan Yan, Hong-Bin Ni, Hai-Hong Huang, Xiao-Dong Lin, Xiao-Yu Liu, Jing-Min Fan, Ming-Sen Zheng, Ru-Ming Yuan\* and Quan-Feng Dong\*

State Key Laboratory of Physical Chemistry of Solid Surfaces, Department of Chemistry, College of Chemistry and Chemical Engineering, Collaborative Innovation Center of Chemistry for Energy Materials (iChEM), Xiamen University, Xiamen, Fujian 361005, China.

<sup>‡</sup>These authors contributed equally to this work

\*Corresponding author e-mail: yuanrm@xmu.edu.cn and qfdong@xmu.edu.cn

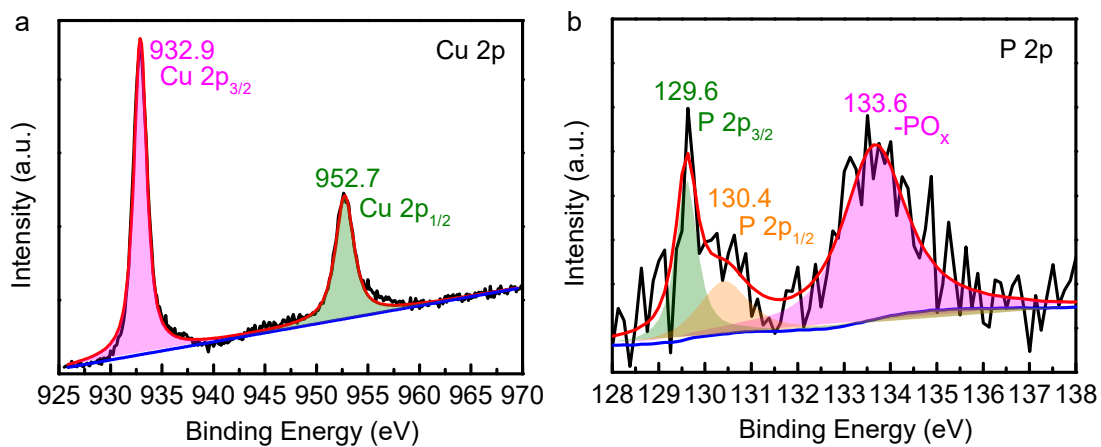


**Fig. S1.** XPS spectra of PCM electrode. (a) Cu 2p, (b) P 2p.

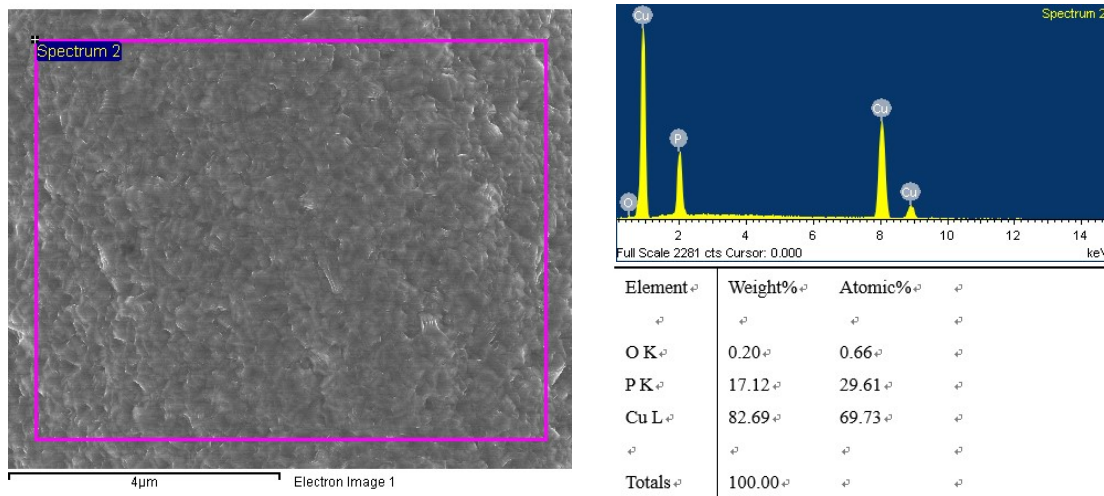


**Fig. S2.** The EDS analysis of PCM electrode.

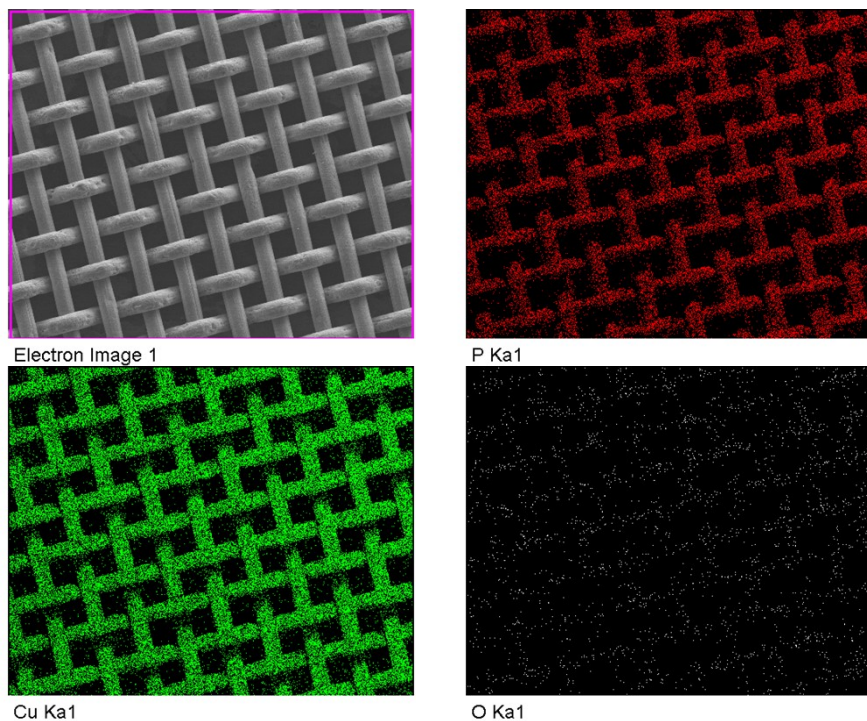


**Fig. S3. The EDX mapping of PCM electrode.**

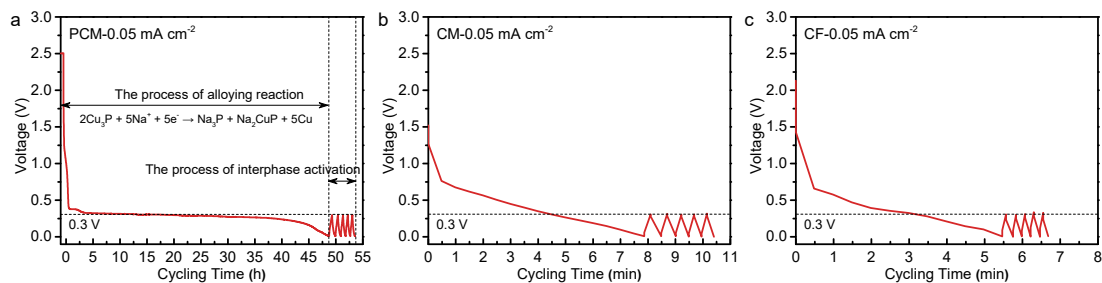


**Fig. S4. Voltage-time plots of various electrodes after initial discharge to 0.01 V at a current density of 0.05 mA cm<sup>-2</sup>.** (a) PCM electrode, (b) CM electrode and (c) CF electrode.

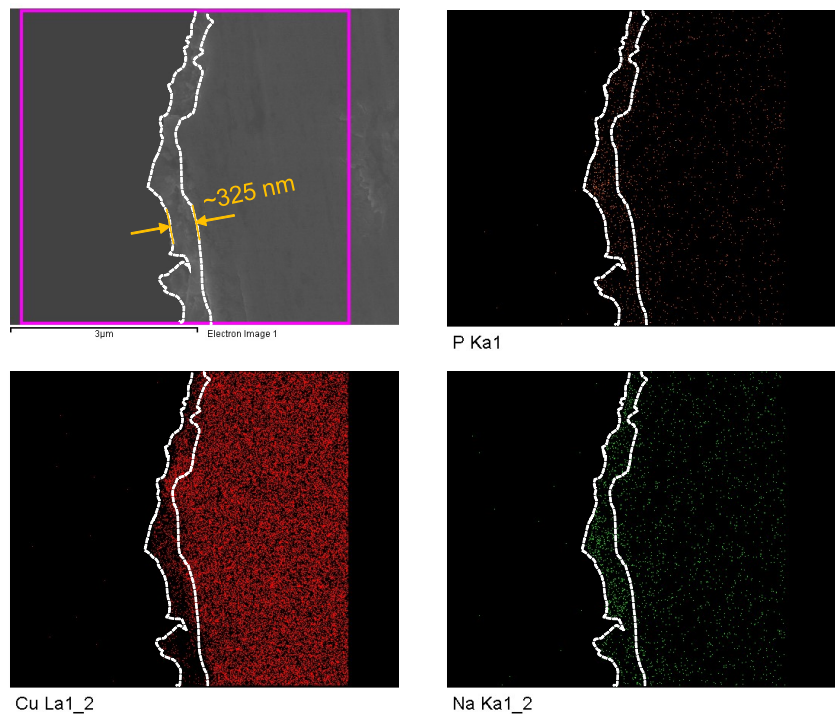


**Fig. S5.** The side-view SEM image and EDX mapping of PCM electrode when discharged to 0.01 V.

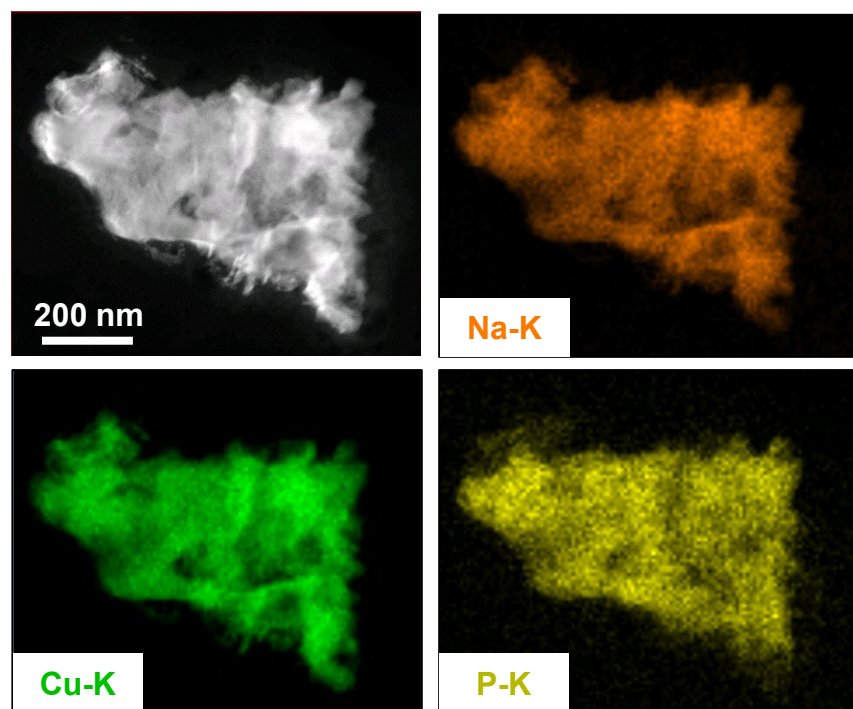


**Fig. S6.** The HAADF-STEM image and elemental mapping of PCM electrode when discharged to 0.01 V.

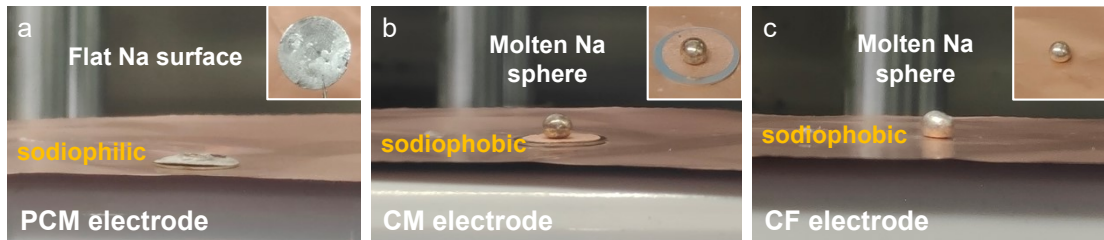


**Fig. S7. The side/top-view optical physical image of molten sodium on different substrates:** (a) PCM electrode, (b) CM electrode and (c) CF electrode. Owing to Cu<sub>3</sub>P can react with Na at high temperature (the temperature is set to 200 °C), which promotes the spontaneous reaction and molten-sodium is continuously attracted until the phosphorized copper mesh is completely infiltrated. The whole process of sodium metal melting and infusing were carried out in a glove box filled with argon (the content of O<sub>2</sub> and H<sub>2</sub>O were kept below 0.1 ppm). Furthermore, the specific process of sodium metal melting and infusing as shown in **Supplementary Video 1** and **Video 2**.

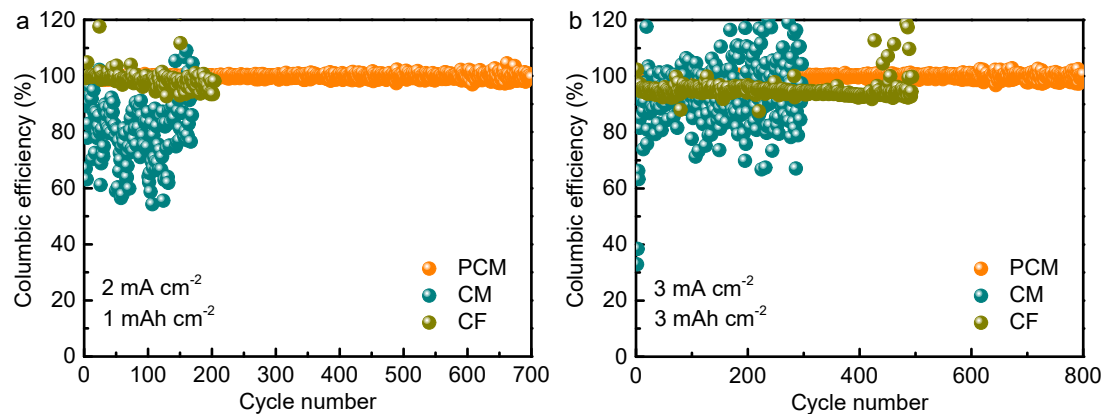


**Fig. S8. Electrochemical cycling stability characterization of PCM, CM and CF electrodes in half-cell.** (a) 2 mA cm<sup>-2</sup>-1 mAh cm<sup>-2</sup>. (b) 3 mA cm<sup>-2</sup>-3 mAh cm<sup>-2</sup>.

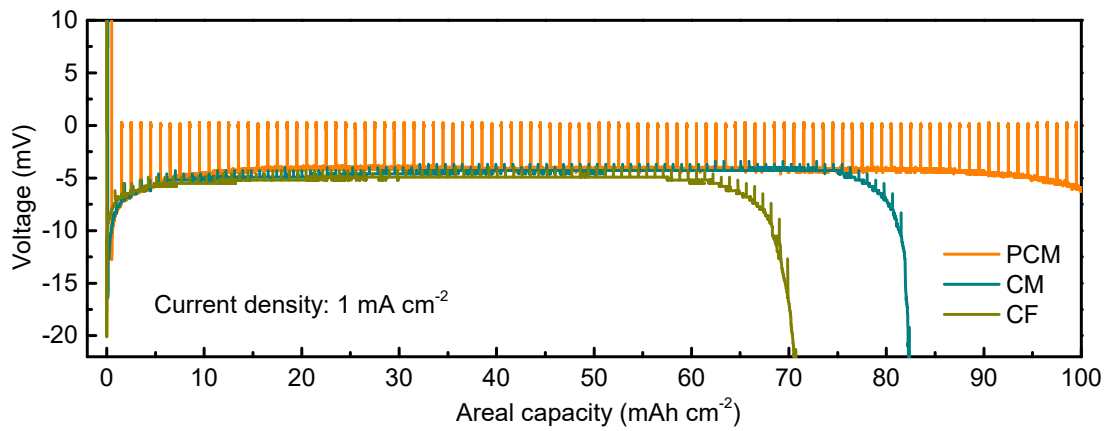


**Fig. S9. Voltage-capacity curves of PCM, CM and CF electrodes during GITT test at a current density of  $1 \text{ mA cm}^{-2}$ .**

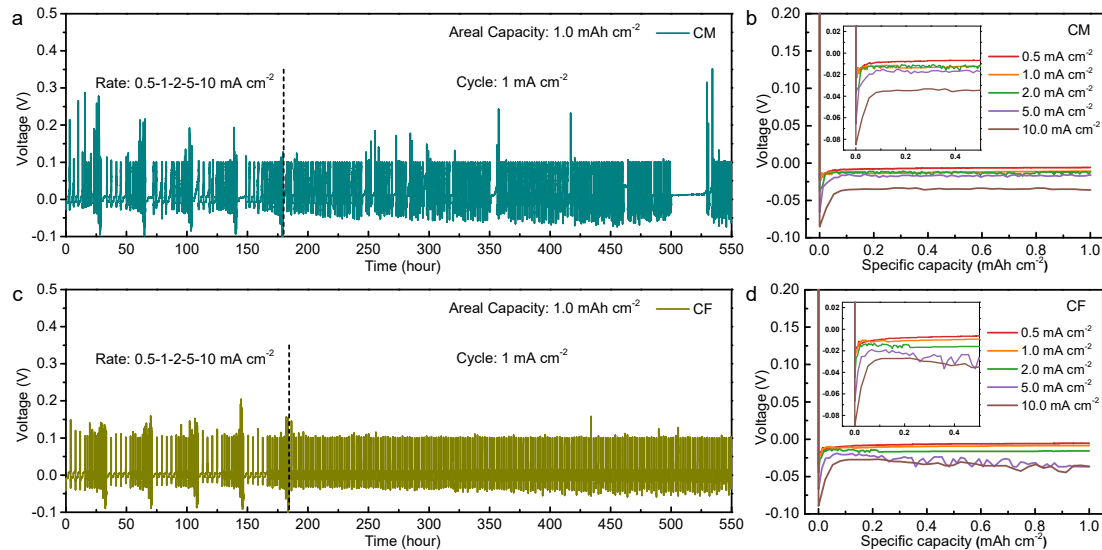


**Fig. S10. Electrochemical rate performance characterization at various current density from 0.5 to 10  $\text{mA cm}^{-2}$  in half-cell.** The voltage-time profiles of (a) CM electrode and (c) CF electrode. The voltage-capacity curves of (b) CM electrode and (d) CF electrode.

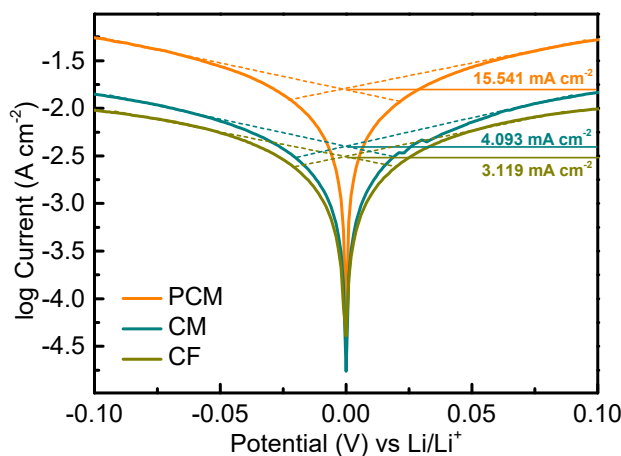


**Fig. S11.** Tafel curves of PCM, CM and CF electrodes.

**Table S1.** The corresponding value of electrodeposition overpotential of PCM, CM and CF electrodes under various current density from 0.5 to 10  $\text{mA cm}^{-2}$  in half-cell.

| Current Collector | Potential (mV) | 0.5 $\text{mA cm}^{-2}$ | 1 $\text{mA cm}^{-2}$ | 2 $\text{mA cm}^{-2}$ | 5 $\text{mA cm}^{-2}$ | 10 $\text{mA cm}^{-2}$ |
|-------------------|----------------|-------------------------|-----------------------|-----------------------|-----------------------|------------------------|
| PCM               | $U_G$          | 2                       | 4                     | 6.5                   | 18                    | 30                     |
|                   | $U_N$          | 5                       | 6                     | 5                     | 6                     | 5                      |
|                   | $U_T$          | 7                       | 10                    | 11.5                  | 24                    | 35.5                   |
| CM                | $U_G$          | 7                       | 11                    | 15                    | 18                    | 34                     |
|                   | $U_N$          | 13                      | 13                    | 23                    | 47                    | 51                     |
|                   | $U_T$          | 20                      | 24                    | 38                    | 65                    | 85                     |
| CF                | $U_G$          | 6                       | 9                     | 15                    | 30                    | 35                     |
|                   | $U_N$          | 28                      | 31                    | 30                    | 32                    | 54                     |
|                   | $U_T$          | 34                      | 40                    | 45                    | 62                    | 89                     |

$U_G = U_{\text{Growth overpotential}}$ ;  $U_N = U_{\text{Nucleation overpotential}}$ ;  $U_T = U_{\text{Tip potential}}$ .

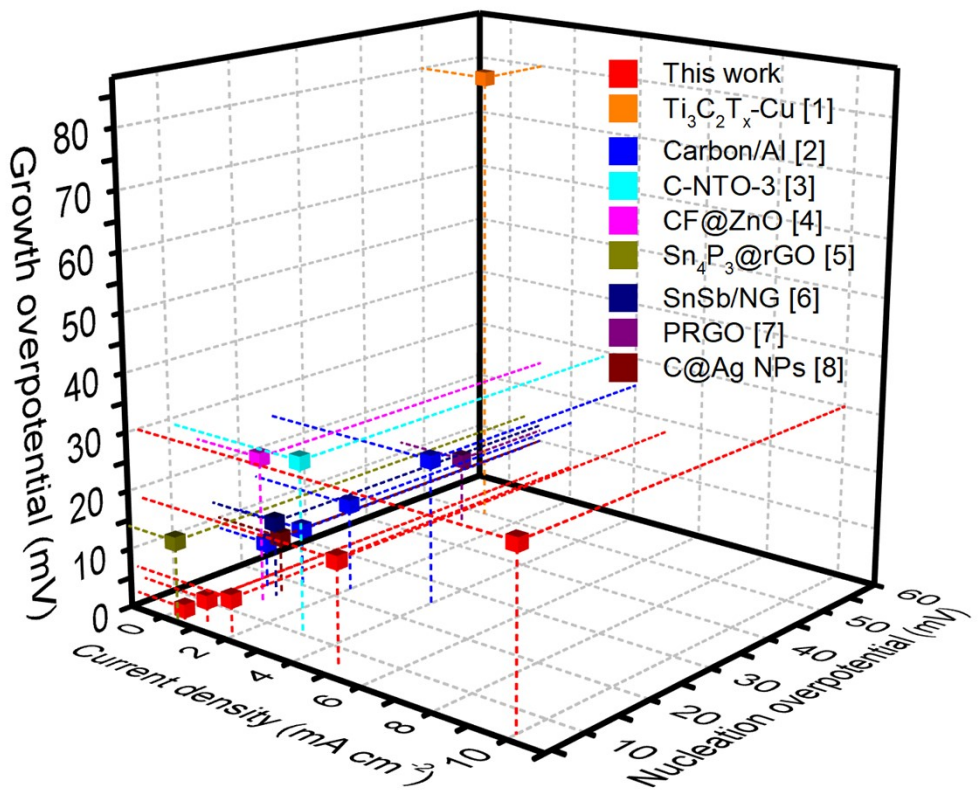


**Fig. S12.** The electrodeposition overpotential of half-cell comparisons between PCM electrode and other previously reported sodium-host skeleton in Na metal anodes.

**Table S2. A comparison of electrodeposition overpotential of half-cell with PCM electrode in this work with some modified skeleton for advanced Na metal anodes in literatures.**

| Current collector                                  | Current density<br>(mA cm <sup>-2</sup> ) | Nucleation<br>overpotential (mV) | Growth overpotential<br>(mV) | Ref.      |
|--|---|----------------------------------|------------------------------|-----------|
| <b>Ti<sub>3</sub>C<sub>2</sub>T<sub>x</sub>-Cu</b> | 1   | 50                               | 80                           | [1]       |
| <b>Carbon/Al</b>                                   | 0.5                                       | 17                               | 8                            | [2]       |
|  | 1   | 20                               | 10                           |           |
|  | 2   | 22.5                             | 15                           |           |
|  | 4   | 25                               | 25                           |           |
| <b>C-NTO-3</b>                                     | 3   | 10.5                             | 29                           | [3]       |
| <b>CF@ZnO</b>                                      | 1   | 14                               | 25                           | [4]       |
| <b>Sn<sub>4</sub>P<sub>3</sub>@rGO</b>             | 0.5                                       | 4                                | 14                           | [5]       |
| <b>SnSb/NG</b>                                     | 1   | 16                               | 13                           | [6]       |
| <b>PRGO</b>  | 1   | 46                               | 12                           | [7]       |
| <b>C@Ag NPs</b>                                    | 1   | 16.8                             | 10                           | [8]       |
| <b>PCM</b>   | 0.5                                       | 5                                | 2                            | This work |
|  | 1   | 6                                | 4                            |           |
|  | 2   | 5                                | 6.5                          |           |
|  | 5   | 6                                | 18                           |           |
|  | 10  | 5.5                              | 30                           |           |

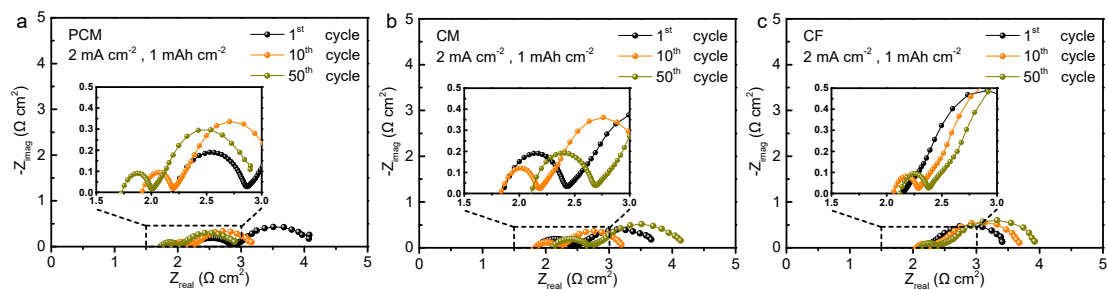


**Fig. S13. The EIS plots of various electrodes measured at 2 mA cm<sup>-2</sup>-1 mAh cm<sup>-2</sup> after 1, 10, 50 cycles. (a) PCM electrode, (b) CM electrode and (c) CF electrode.**

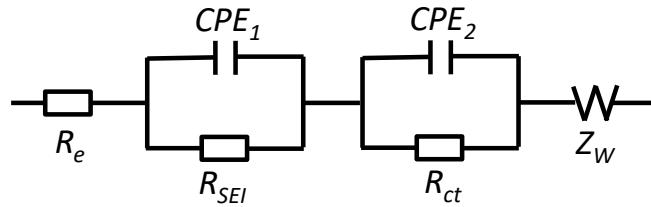


**Fig. S14.** The equivalent circuit of the EIS test.

**Table S3.** The Equivalent Circuit Fitting results of EIS measurements of PCM, CM and CF electrodes.

| Current Collector | Cycle                | $R_e(\Omega)$ | $R_{SEI}(\Omega)$ | $R_{ct}(\Omega)$ |
|-------------------|----------------------|---------------|-------------------|------------------|
| PCM               | After the 1st cycle  | 2.09          | 0.75              | 1.43             |
|                   | After the 10th cycle | 1.91          | 0.29              | 1.04             |
|                   | After the 50th cycle | 1.72          | 0.28              | 0.99             |
| CM                | After the 1st cycle  | 1.82          | 0.62              | 1.52             |
|                   | After the 10th cycle | 1.81          | 0.38              | 1.12             |
|                   | After the 50th cycle | 2.10          | 0.63              | 1.59             |
| CF                | After the 1st cycle  | 2.13          | 0.87              | 0.45             |
|                   | After the 10th cycle | 2.05          | 0.23              | 1.56             |
|                   | After the 50th cycle | 2.10          | 0.29              | 1.69             |

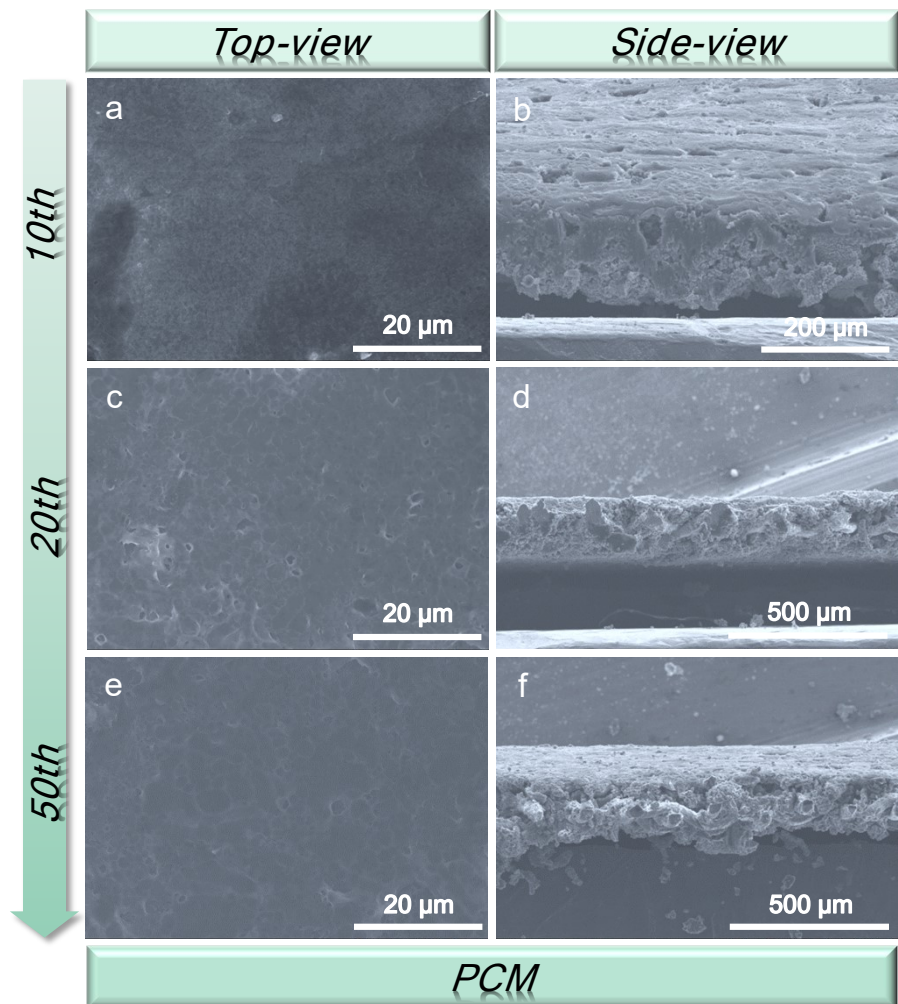


**Fig. S15. High magnification top-view and side-view SEM images of deposited Na for after various cycles at  $1 \text{ mA cm}^{-2}$ - $1 \text{ mAh cm}^{-2}$  on PCM electrode. (a-b) 10th cycle (c-d) 20th cycle and (e-f) 50th cycle.**

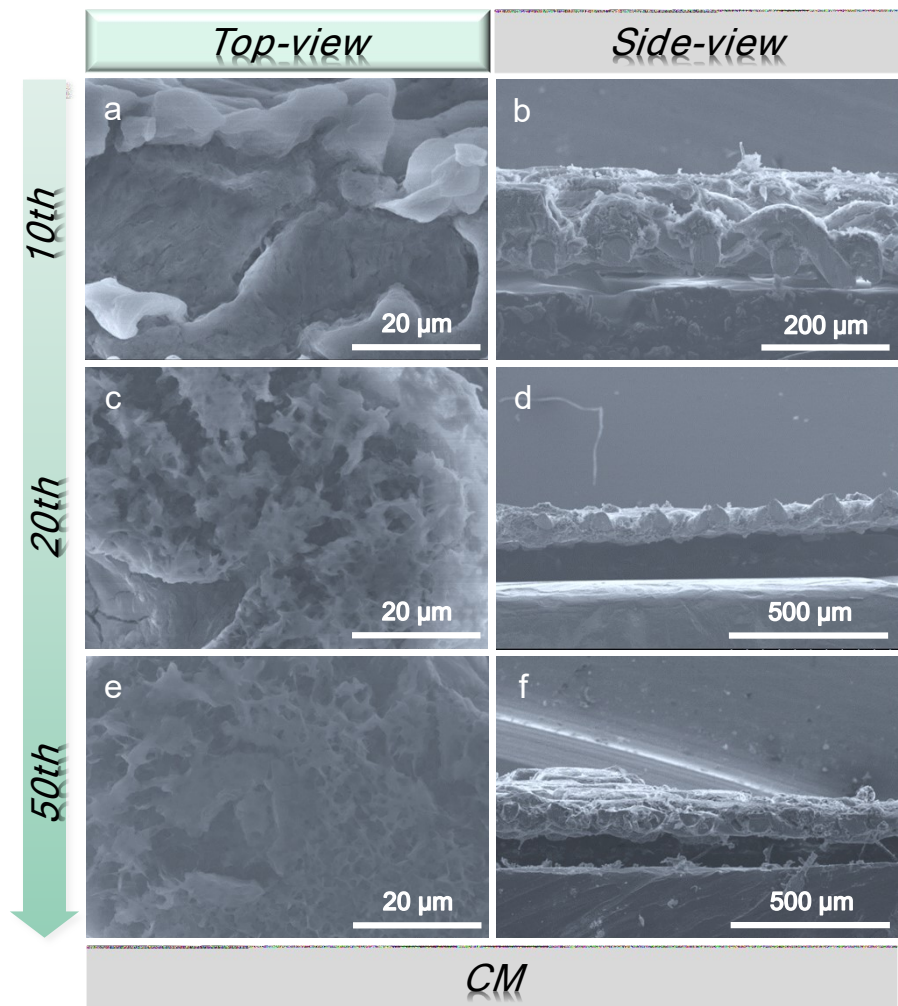


**Fig. S16. High magnification top-view and side-view SEM images of deposited Na for after various cycles at  $1 \text{ mA cm}^{-2}$ - $1 \text{ mAh cm}^{-2}$  on CM electrode. (a-b) 10th cycle (c-d) 20th cycle and (e-f) 50th cycle.**

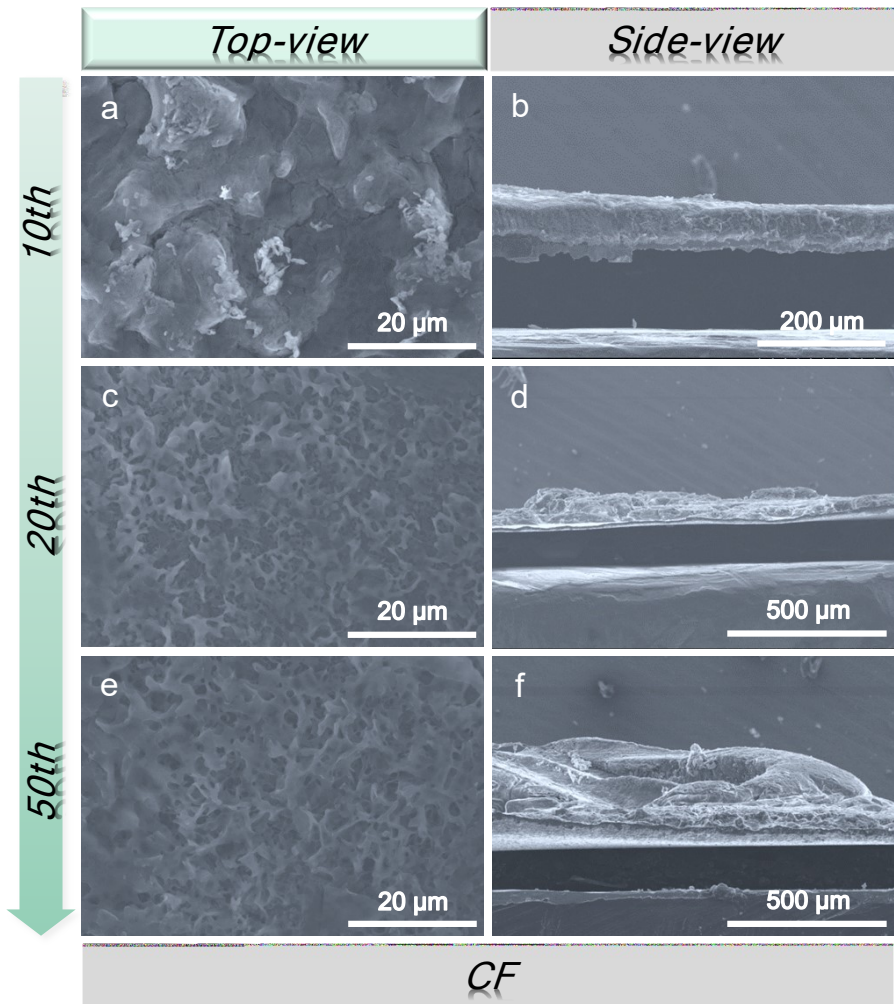


**Fig. S17. High magnification top-view and side-view SEM images of deposited Na for after various cycles at  $1 \text{ mA cm}^{-2}$ - $1 \text{ mAh cm}^{-2}$  on CF electrode. (a-b) 10th cycle (c-d) 20th cycle and (e-f) 50th cycle.**

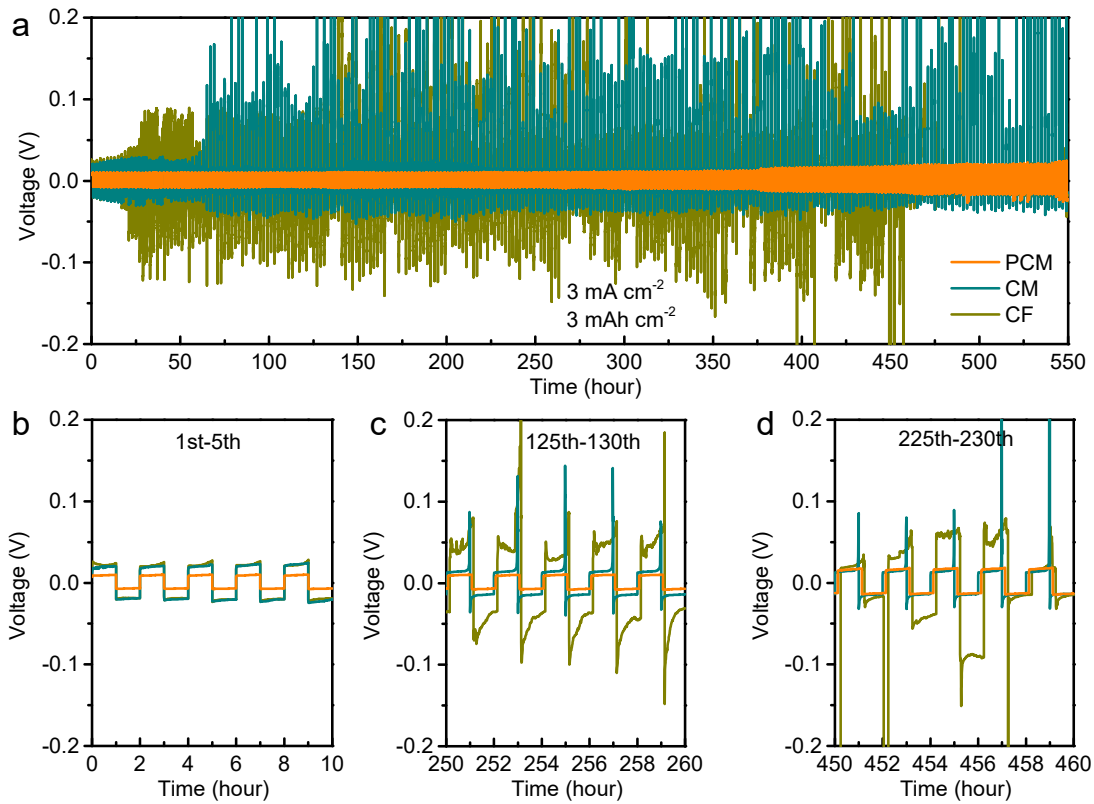


**Fig. S18. Electrochemical long-term cycling performance of symmetric-cell.** (a) The rate capabilities of PCM@Na||PCM@Na, CM@Na||CM@Na, CF@Na||CF@Na symmetric-cell at 3  $\text{mA cm}^{-2}$ -3  $\text{mAh cm}^{-2}$ . Magnified voltage-time profiles of (a) during (b) 0~10 h; (c) 250~260 h; (d) 450~460 h.

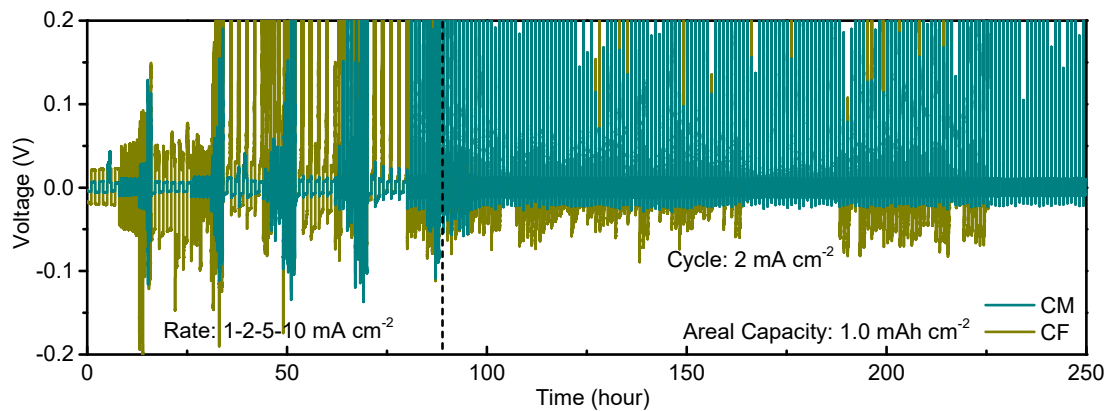


**Fig. S19. Electrochemical rate capabilities performance of CM@Na||CM@Na, CF@Na||CF@Na symmetric-cell.**

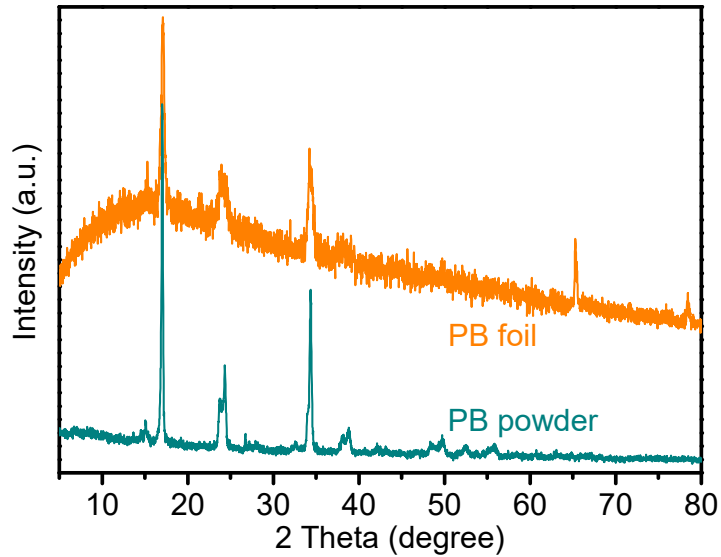


**Fig. S20. The XRD patterns of Prussian blue (PB) power and aluminum foil with PB (i.e. PB foil).** The alignment of the peak positions indicates that the PB remains unchanged after being slurried and coated on the aluminum foil.

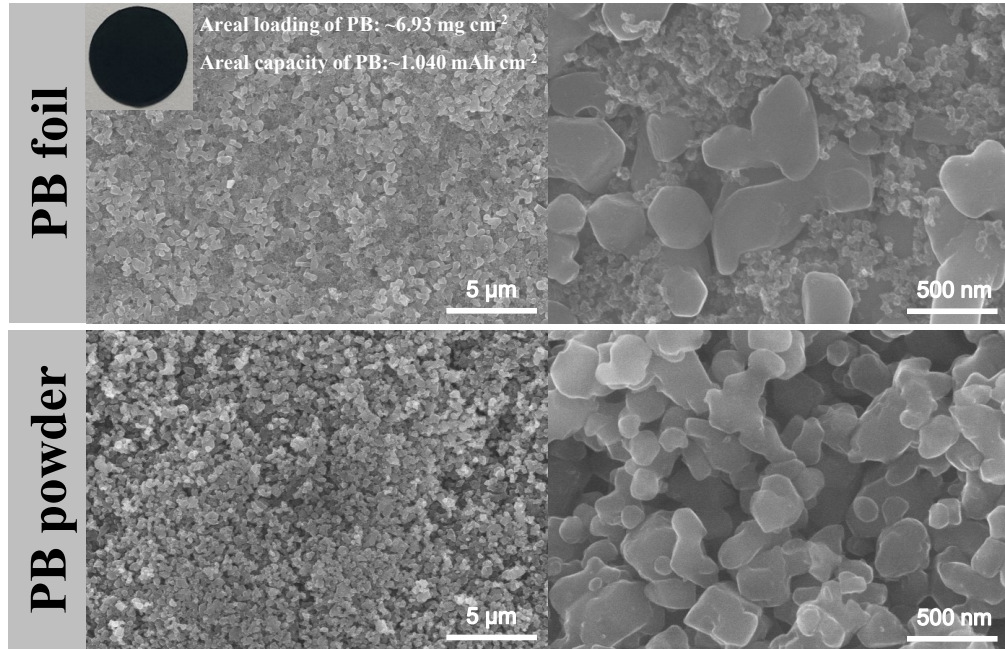


**Fig. S21. The SEM images of Prussian blue (PB) power and aluminum foil with PB (i.e. PB foil).** Among them, the morphology of PB remains unchanged after being slurried and coated on the aluminum foil. For PB foil, the areal loading of PB is about  $6.93 \text{ mg cm}^{-2}$ .

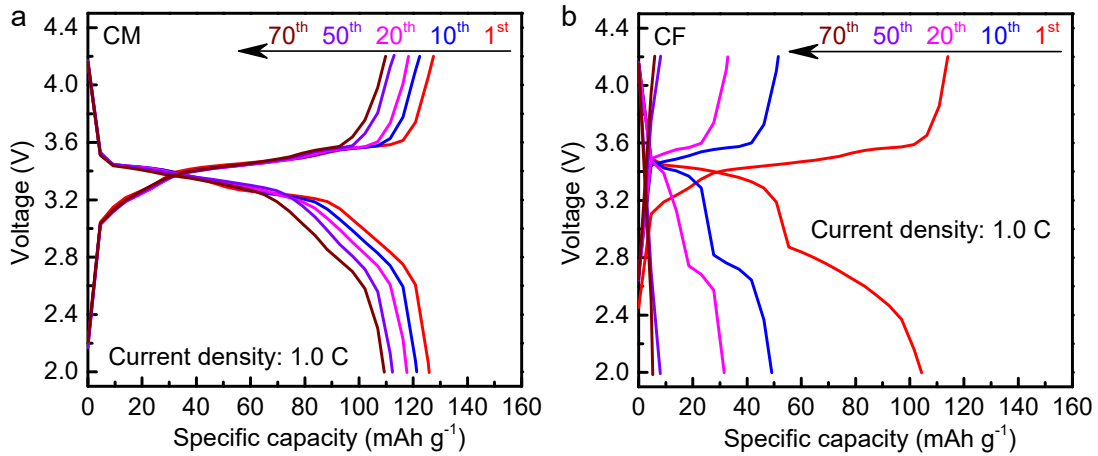


**Fig. S22. The various selected voltage-capacity curves of (a) CM@Na||PB and (b) CF@Na||PB full-cell.**

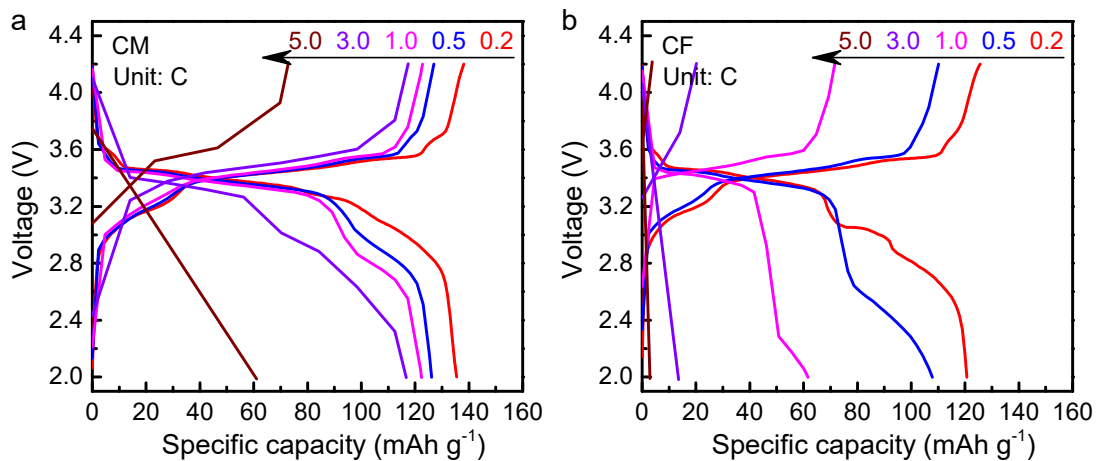


**Fig. S23. The selected voltage-capacity curves of (a) CM@Na||PB and (b) CF@Na||PB full-cell at different rates.**



**Fig. S24.** LED lights (48 pcs) powered by one PCM@Na||PB full-cell for 5 s, 1 min, 5 min, 10 min, 15 min and 20 min.

## Reference

- [1] Y. Fang, R. Lian, H. Li, Y. Zhang, Z. Gong, K. Zhu, K. Ye, J. Yan, G. Wang, Y. Gao, Y. Wei and D. Cao, *ACS Nano*, 2020, **14**, 8744-8753.
- [2] A. P. Cohn, N. Muralidharan, R. Carter, K. Share and C. L. Pint, *Nano Lett.*, 2017, **17**, 1296-1301.
- [3] J. Luo, X. Lu, E. Matios, C. Wang, H. Wang, Y. Zhang, X. Hu and W. Li, *Nano Lett.*, 2020, **20**, 7700-7708.
- [4] W. Yang, W. Yang, L. Dong, G. Shao, G. Wang and X. Peng, *Nano Energy*, 2021, **80**, 105563.
- [5] M. Bai, Y. Liu, K. Zhang, X. Tang, S. Liu and Y. Ma, *Energy Storage Mater.*, 2021, **38**, 499-508.
- [6] Z. Wang, K. Lu, F. Xia, O. Dahunsi, S. Gao, B. Li, R. Wang, S. Lu, W. Qin, Y. Cheng and X. Wu, *J. Mater. Chem. A*, 2021, **9**, 6123-6130.
- [7] K. Yan, S. Zhao, J. Zhang, J. Safaei, X. Yu, T. Wang, S. Wang, B. Sun and G. Wang, *Nano Lett.*, 2020, **20**, 6112-6119.
- [8] N. Zhu, X. Mao, G. Wang, M. Zhu, H. Wang, G. Xu, M. Wu, H. K. Liu, S.-X. Dou and C. Wu, *J. Mater. Chem. A*, 2021, **9**, 13200-13208.